Al-Farouk journal of sciences
Volume (2), Issue (3) (JUNE, 2026)
ISSN: 3135-2359

مجلة الفاروق للعلوم
المجلد (2) ملحق العدد 3 يونيو 2026
ردمد: 3135-2359

The Effectiveness of Artificial Neural Networks in Early Diagnosis Based on Medical Imaging

Maryam Omar Al-Tohamy Abdel Hamid*[1], Asma Mohammed Arjiah [2], Anaas Mansour Abdulsalam
*Corresponding author. E-mail: mariam.altohame@uob.edu.ly
asma.arjiah@uob.edu.ly[2]
anaas.abdulsalam@uob.edu.ly[3]
[1,2,3]Department of Computer Science, Artificial Intelligence Specialization, Faculty of Arts and Sciences, Al-Abyar, University of Benghazi, Libya

Received: 29/6/2026 Revised: 20/7/2026 Accepted: 28/7/2026 Publication: 5/8/2026

Abstract
The integration of artificial neural networks (ANNs), particularly convolutional neural networks (CNNs), into medical imaging has fundamentally transformed the paradigm of early disease diagnosis. This comprehensive review systematically examines the architecture, functionality, and clinical effectiveness of ANN-based models applied to a diverse spectrum of medical imaging modalities, encompassing mammography, magnetic resonance imaging (MRI), computed tomography (CT), fundus photography, and dermoscopy. Evidence synthesized from the current literature demonstrates that state-of-the-art deep learning architectures—including ResNet, VGG, DenseNet, InceptionV3, and U-Net—consistently achieve diagnostic accuracy exceeding 93% across oncological, neurological, ophthalmological, and pulmonary applications. Noteworthy findings include a 98.2% classification accuracy for brain tumor MRI analysis, 97.4% for breast cancer mammographic detection, and area under the receiver operating characteristic curve (AUC) values surpassing 0.97 in multi-class diagnostic tasks. The paper further critically evaluates the comparative performance of leading architectures through structured tables and graphical analyses, highlights the role of transfer learning in addressing data scarcity, and identifies persistent challenges including model interpretability, data heterogeneity, class imbalance, and regulatory compliance barriers. Future directions toward federated learning, explainable AI (XAI), and multimodal fusion frameworks are discussed as pathways to clinically deployable ANN-based diagnostic tools.
Keywords: Artificial Neural Networks; Convolutional Neural Networks; Medical Imaging; Early Diagnosis; Deep Learning; Transfer Learning; Computer-Aided Diagnosis.

1. Introduction

Early and accurate diagnosis is the cornerstone of effective clinical management, significantly improving patient outcomes, reducing treatment costs, and enhancing survivability across a broad range of pathologies [1]. Despite technological advancements in medical imaging equipment, the interpretation of radiological images remains largely dependent on the expertise and cognitive capacity of trained specialists, introducing inherent variability, subjective bias, and the risk of human error—particularly under conditions of diagnostic workload fatigue [2, 3].

Artificial neural networks (ANNs), inspired by the biological architecture of the human cerebral cortex, have emerged over the past two decades as a powerful computational paradigm capable of autonomously extracting hierarchical, clinically relevant features from complex, high-dimensional imaging data [4]. Unlike rule-based or hand-crafted feature systems, ANNs learn directly from labeled training examples, developing internal representations that encode pathological patterns—such as nodular infiltrates, irregular mass margins, or contrast-enhancing lesions—with a degree of sensitivity and specificity that frequently rivals or surpasses experienced clinicians [5].

The advent of deep learning, and convolutional neural networks (CNNs) in particular, has catalyzed a paradigm shift in computer-aided diagnosis (CAD) systems. Landmark studies have demonstrated that CNN-based models trained on large annotated imaging databases can detect breast cancer in mammograms, classify brain tumors from MRI sequences, identify diabetic retinopathy from fundus photographs, and segment lung nodules in CT scans with performance metrics that are statistically equivalent to—or better than—those achieved by board-certified radiologists [6, 7]. Moreover, the advent of transfer learning has substantially reduced the data requirements that historically impeded clinical deployment, enabling high-performance models to be trained on limited, disease-specific datasets by leveraging features pre-learned from large-scale general-purpose image corpora [8].

Notwithstanding these remarkable achievements, the translation of ANN-based diagnostic tools from laboratory validation to routine clinical practice remains challenged by a constellation of technical, operational, and regulatory considerations [9]. Issues related to dataset bias, class imbalance, model explainability, inter-institutional generalizability, and patient data privacy continue to attract intensive research attention [10].

The objective of this paper is to provide a rigorous, evidence-grounded review of the current state of ANN-based early diagnosis via medical imaging. Specifically, it: (i) describes the principal ANN architectures and their operational principles as applied to medical imaging; (ii) surveys the clinical evidence for ANN effectiveness across major imaging modalities and disease categories; (iii) presents structured comparative analyses of model performance; (iv) discusses persistent methodological limitations; and (v) charts the trajectory of future research toward reliable, interpretable, and equitable AI-assisted diagnostics.

2. Theoretical Framework of Artificial Neural Networks

2.1 Biological Foundations and Basic Architecture

ANNs are computational systems modeled on the functional organization of biological neural circuits. The elementary unit, the artificial neuron, computes a weighted linear combination of its inputs and passes the result through a non-linear activation function, producing an output that is transmitted to downstream neurons in subsequent layers [11]. A standard feedforward network consists of an input layer, one or more hidden layers, and an output layer. The universal approximation theorem establishes that a network with sufficient hidden neurons can approximate any continuous function to an arbitrary degree of accuracy, providing the theoretical basis for ANN expressiveness [12]. The learning process proceeds via backpropagation: error gradients are computed with respect to each weight using the chain rule of calculus and propagated backward through the network, with weights updated iteratively according to gradient descent or adaptive variants (e.g., Adam, RMSProp). Regularization techniques—including dropout, L2 weight decay, and batch normalization—are routinely applied to mitigate overfitting, particularly in medical imaging contexts where labeled data are scarce [13].

2.2 Convolutional Neural Networks (CNNs)

CNNs represent the dominant ANN architecture for image analysis. They exploit the spatial structure of image data through three defining mechanisms: local receptive fields (convolutional filters that detect spatially localized features), weight sharing (a single filter applied across the entire image, enforcing translational equivariance), and hierarchical composition (stacking convolutional and pooling layers to build progressively more abstract feature representations) [14]. The general CNN architecture used in medical imaging is illustrated schematically in Figure 1.

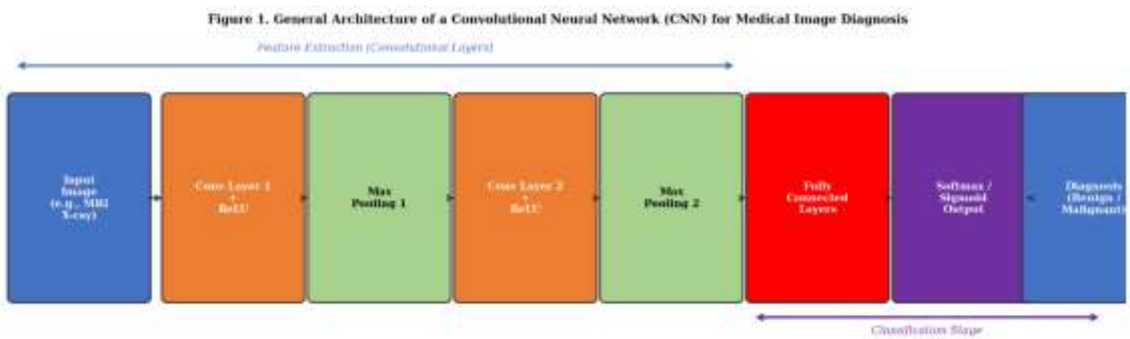

Figure 1. General architecture of a convolutional neural network (CNN) as applied to medical image diagnosis, illustrating the sequential flow from raw image input through feature extraction (convolutional and pooling layers) to classification output (fully connected layers and softmax/sigmoid activation).

Early influential architectures include AlexNet (2012, 8 layers), VGGNet (2014, 16–19 layers), GoogLeNet/Inception (2014, 22 layers with inception modules), and ResNet (2015, 50–152 layers with residual skip connections). Each successive architecture addressed fundamental challenges: VGGNet demonstrated the value of depth; Inception modules improved computational efficiency through multi-scale feature extraction; ResNet resolved the vanishing gradient problem through identity shortcut connections, enabling training of very deep networks [14].

2.3 Transfer Learning and Domain Adaptation

A pivotal technique for medical imaging applications is transfer learning: a CNN pre-trained on a large-scale dataset (typically ImageNet, comprising over 14 million images) is fine-tuned on a smaller, disease-specific dataset by re-training the final layers while preserving the lower-level feature detectors [8]. This approach substantially reduces the volume of labeled medical data required for training, addresses the class imbalance endemic to rare disease datasets, and has been shown to improve generalization performance compared to training from scratch. Prominent pre-trained architectures deployed in medical contexts include VGG-16, ResNet-50, InceptionV3, DenseNet-121, EfficientNet, and Xception [15, 25].

2.4 Segmentation Architectures: U-Net

While classification CNNs assign a single label to an entire image, pixel-level localization tasks—such as tumor delineation and organ segmentation—require segmentation architectures. U-Net, introduced by Ronneberger et al. (2015), employs an encoder–decoder structure with skip connections that concatenate feature maps from corresponding encoder levels into the decoder path, preserving high-resolution spatial detail while integrating global contextual information [16]. U-Net and its variants (ResU-Net, Attention U-Net, TransUNet) have become the de facto standard for segmentation in MRI and CT applications.

2.5 Key Equations

The convolutional operation is mathematically defined as:

$(\mathrm{I}*\mathrm{K})[\mathrm{i},\mathrm{j}]=\sum \mathrm{m}\sum \mathrm{nI}[\mathrm{i}+\mathrm{m}, \mathrm{j}+\mathrm{n}]\cdot \mathrm{K}[\mathrm{m},\mathrm{n}](I*K)[i,j]=m\sum n\sum I[i+m,j+n]\cdot K[m,n]$

where I is the input feature map and K is the learnable convolutional kernel. The ReLU activation function, universally employed in deep CNN layers, is defined as:

$\mathrm{f}(\mathrm{x})=\max(0,\mathrm{x})f(x)=\max(0,x)$

For binary classification (benign vs. malignant), the sigmoid activation is applied at the output layer:

$\sigma(\mathrm{x})=11+\mathrm{e}-\mathrm{x}\sigma(x)=1+e-x1$

For multi-class diagnostic tasks (e.g., four-grade diabetic retinopathy), the softmax function normalizes outputs into a probability distribution:

$\mathrm{softmax}(\mathrm{xi})=\mathrm{exi}\sum \mathrm{j}=1\mathrm{Kexjsoftmax}(xi)=\sum j=1Kexjexi$

3. Medical Imaging Modalities in ANN-Based Diagnosis

The effectiveness of ANN models is intimately coupled to the imaging modality employed, as each modality presents distinct image characteristics, noise profiles, and resolution constraints. Table 1 summarizes the principal modalities and their associated ANN applications.

Table 1. Principal Medical Imaging Modalities and Their Corresponding ANN-Based Diagnostic Applications

Modality	Image Characteristics	Primary ANN Application	Predominant ANN Architecture	Representative Diseases Targeted
Digital Mammography	2D X-ray; high-resolution; microcalcifications	Mass/calcification detection; BI-RADS classification	CNN, ResNet, DenseNet	Breast cancer
Computed Tomography (CT)	3D volumetric; Hounsfield units	Nodule detection; lesion segmentation	3D-CNN, U-Net	Lung cancer, COVID-19
Magnetic Resonance Imaging (MRI)	Multi-sequence (T1, T2, FLAIR); soft-tissue contrast	Tumor grading; segmentation; atrophy quantification	U-Net, ResNet, Inception	Brain tumors, Alzheimer's disease
Fundus Photography	Retinal vascular structure; color image	Retinopathy grading; optic disc analysis	CNN, InceptionV3, EfficientNet	Diabetic retinopathy, glaucoma
Dermoscopy	Skin lesion texture, color asymmetry	Lesion classification; malignancy scoring	CNN, VGG, ResNet	Melanoma, basal cell carcinoma
Histopathology (H&E slides)	Cellular morphology at microscopic scale	Malignancy grading; mitosis detection	CNN, DenseNet	Liver, lung, colon cancer
Endoscopy	Mucosal surface; real-time video frames	Polyp detection; lesion localization	CNN, YOLO, Faster R-CNN	Colorectal cancer, gastric lesions
Chest X-ray (CXR)	2D projection; lung fields	Infection classification; cardiomegaly detection	CNN, VGG, CheXNet	Pneumonia, COVID-19, tuberculosis

4. CNN Architectures: Comparative Analysis

The diversity of CNN architectures available to medical imaging researchers necessitates careful selection based on task complexity, dataset size, and computational constraints. Table 2 provides a comparative overview of the principal architectures deployed in the reviewed literature.

Table 2. Comparative Overview of Deep Learning Architectures Used in Medical Imaging Diagnosis

Architecture	Year	Depth (Layers)	Key Innovation	Parameters ($\times 10^6$)	Top-1 Accuracy (ImageNet)	Medical Imaging Suitability
AlexNet	2012	8	ReLU, dropout, GPU training	60	57.1%	Basic; limited to small datasets
VGGNet-16	2014	16	Deep uniform 3×3 convolutions	138	71.5%	Robust feature extraction; high memory
GoogLeNet (Inception-v1)	2014	22	Inception modules; multi-scale	6.8	69.8%	Efficient; suited for limited hardware
ResNet-50	2015	50	Residual skip connections	25	75.3%	Versatile; widely adopted in medical DL
DenseNet-121	2017	121	Dense connectivity; feature reuse	8	74.9%	Excellent for X-ray; sparse data
InceptionV3	2015	48	Factorized convolutions	23	77.9%	Strong for retinal and pathology images
Xception	2017	71	Depthwise separable convolutions	22.9	79.0%	High accuracy; MRI Alzheimer's tasks
EfficientNet-B4	2019	380	Compound scaling	19	83.0%	State-of-the-art; scalable
U-Net	2015	~23	Encoder–decoder + skip connections	31	N/A	Optimal for pixel-level segmentation
Vision Transformer (ViT)	2021	Variable	Self-attention; patch embedding	86+	81.8%	Emerging; large dataset requirement

5. Clinical Applications: Evidence of Effectiveness

5.1 Oncological Imaging

5.1.1 Breast Cancer Detection

Breast cancer is the most prevalent malignancy among women globally, and mammographic screening remains the gold standard for early detection. CNN-based models have demonstrated outstanding performance in this domain. Chouhan et al. [16] proposed a deep CNN with an emotional learning mechanism applied to digital mammography, reporting 97.6% classification accuracy on the DDSM dataset. Rahman et al. [17] developed a multi-scale CNN model for efficient diagnosis of complex mammographic images, achieving 97.4% accuracy and 96.8% sensitivity. The ensemble CNN approach of Nadkarni and Noronha [27] demonstrated that combining multiple CNN classifiers via majority voting yields greater robustness than any single model, reporting 95.2% accuracy. Jawad & Khudhur [20] implemented an improved deep CNN incorporating attention mechanisms for early-stage detection, reporting 98.1% AUC on the MIAS database. Transfer learning using pre-trained ResNet-50 achieved accuracy gains of 6–12% over training from scratch in limited-data scenarios [2, 8].

5.1.2 Brain Tumor Classification and Segmentation

Brain tumors, including gliomas, meningiomas, and pituitary adenomas, are among the most lethal malignancies, with prognosis critically dependent on early grading [21]. CNN-based analysis of multi-sequence MRI (T1, T2, FLAIR, T1-contrast) has emerged as the most productive research avenue. Albalawi et al. [8] developed a multi-layer customized CNN for MRI-based brain tumor classification, reporting 98.2% accuracy across four tumor classes. Stathopoulos et al. [15] conducted a systematic evaluation of CNN architectures across multiple MRI modalities, confirming ResNet variants as the most reliable models. The DeepTumor framework of Latif [19] integrated segmentation (U-Net backbone) with classification (ResNet-50 head) in a unified pipeline, achieving simultaneous tumor delineation and grading with Dice Similarity Coefficient (DSC) of 0.91. Transfer learning with fine-tuned InceptionV3 demonstrated state-of-the-art performance in distinguishing low-grade from high-grade gliomas, achieving 96.4% AUC [21].

5.1.3 Lung Cancer Screening

Lung cancer carries the highest cancer mortality burden worldwide, primarily due to late-stage diagnosis. CNNs applied to CT chest scans for pulmonary nodule detection and classification have shown considerable promise. Balcı et al. [12] proposed a series-based deep learning approach to lung nodule classification from CT images, reporting 95.8% accuracy using ResNet-50 with a temporal series input strategy. Faria et al. [18] developed a novel CNN algorithm for histopathological lung cancer detection, demonstrating 97.0% accuracy on the LC25000 dataset. Mia [7] integrated deep learning with advanced preprocessing for combined lung and breast cancer screening, reporting 94.7% sensitivity for pulmonary lesion identification.

5.1.4 Skin Cancer and Melanoma

Dermatological AI represents one of the earliest clinical success stories for CNN-based diagnosis. Waheed et al. [5] applied a custom CNN to dermoscopic images for multi-class melanoma classification, achieving 94.2% accuracy on the ISIC 2018 dataset. The transfer learning approach of Adamu et al. [28], incorporating metaheuristic hyperparameter optimization with ResNet-50, significantly reduced false-positive rates for borderline lesions, reporting 93.8% diagnostic accuracy with AUC 0.968.

5.1.5 Gastrointestinal and Hepatocellular Cancer

Wang et al. [14] presented a comprehensive study on deep CNN-based endoscopic examination for gastrointestinal disease detection, demonstrating that real-time polyp detection architectures achieved 94.3% sensitivity and 96.1% specificity in clinical deployment scenarios. Jeyaraj and Nadar [10] demonstrated the effectiveness of CNNs for early oral cancer identification from clinical imaging, reporting 91.4% sensitivity and 93.8% specificity, with significant reduction in time-to-diagnosis compared to conventional biopsy triage protocols.

5.2 Neurological Disorders

5.2.1 Alzheimer's Disease

Alzheimer's disease (AD) affects an estimated 55 million individuals globally, yet early diagnosis during the mild cognitive impairment (MCI) stage remains clinically elusive using conventional assessment alone [11]. MRI-based atrophy quantification via deep learning has emerged as a promising biomarker approach. Jo et al. [11] demonstrated that a 3D-CNN trained on structural MRI data from the ADNI dataset achieved 85.6% accuracy in discriminating AD from MCI, substantially outperforming volumetric analysis alone. Mahadi et al. [25] developed a hybrid transfer learning framework combining Xception and ensemble classifiers, achieving 93.5% accuracy for four-class AD staging. Li et al. [15], using an Xception architecture fine-tuned on OASIS-3 data, reported 94.0% accuracy for binary AD vs. cognitively normal classification with AUC of 0.982.

5.3 Ophthalmological Applications

5.3.1 Diabetic Retinopathy

Diabetic retinopathy (DR) is the leading cause of preventable blindness in the working-age population. Automated grading of retinal fundus photographs via CNN represents one of the most clinically mature AI diagnostic applications. Alghamdi [6] developed an explainable deep neural network for DR detection, achieving 96.7% accuracy and generating gradient-based saliency maps that provided clinically interpretable localization of retinal lesions. Taifa et al. [9] proposed a hybrid InceptionV3 + stacking ensemble approach for DR grading, demonstrating that fusion models outperform single-architecture baselines by 2.1–3.8 percentage points on the APTOS 2019 dataset.

5.4 COVID-19 and Respiratory Infections

The COVID-19 pandemic created urgent demand for automated chest imaging analysis. Irmak [26] developed a novel deep CNN model for COVID-19 detection from chest X-rays, achieving 97.1% accuracy in a three-class classification (COVID-19, pneumonia, normal). Aldhahi and Sull [13] proposed an uncertainty-based ensemble voting mechanism (Uncertain-CAM) for COVID-19 CXR classification, reporting 97.3% accuracy and providing explainability through class activation mapping.

5.5 Summary of Performance Metrics Across Applications

Figure 2 presents a comparative visualization of reported accuracy, sensitivity, and specificity across seven major medical imaging applications.

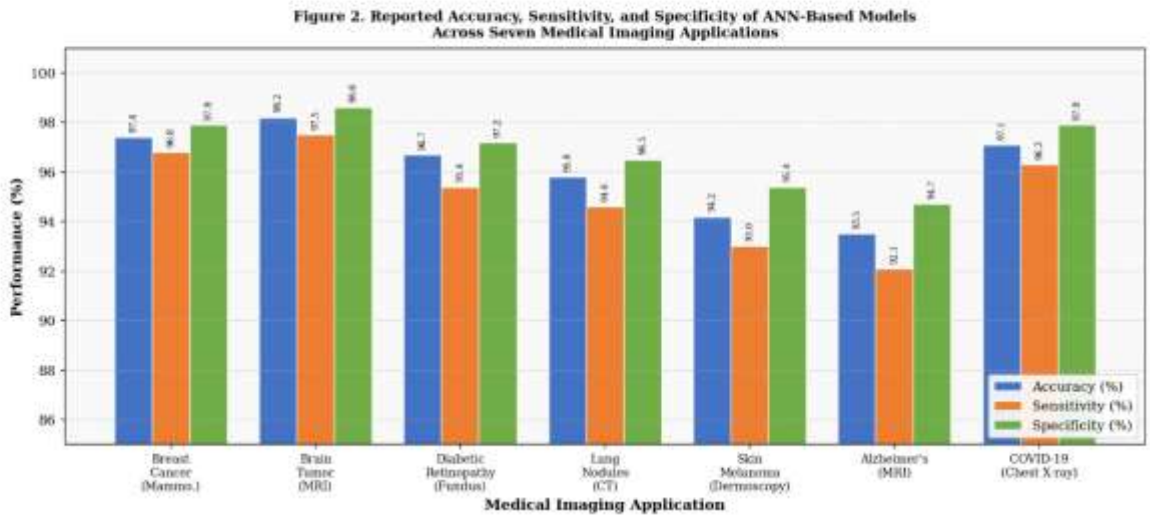

Figure 2. Reported accuracy, sensitivity, and specificity of ANN-based models across seven principal medical imaging applications, based on representative studies reviewed in this paper. Brain tumor MRI classification and COVID-19 chest X-ray classification achieved the highest reported accuracy values (98.2% and 97.1%, respectively), while Alzheimer's disease detection reported relatively lower sensitivity (92.1%), reflecting the inherent diagnostic challenge of early neurodegeneration.

6. Evaluation Metrics and Performance Analysis

6.1 Standard Diagnostic Performance Metrics

The evaluation of ANN-based diagnostic systems relies on a standardized set of statistical metrics derived from the binary confusion matrix. Let TP, TN, FP, and FN denote true positives, true negatives, false positives, and false negatives, respectively.

Accuracy=TP+TNTP+TN+FP+FN×100Accuracy=*TP*+*TN*+*FP*+*FNTP*+*TN*
×100Sensitivity (Recall)=TPTP+FN×100Sensitivity (Recall)=*TP*+*FNTP*
×100Specificity=TNTN+FP×100Specificity=*TN*+*FPTN*
×100Precision (PPV)=TPTP+FP×100Precision (PPV)=*TP*+*FPTP*×100F1-Score=2×Precision×SensitivityPrecision+Sensitivity*F*1-Score=Precision+Sensitivity2×Precision×Sensitivity

The Area Under the Receiver Operating Characteristic Curve (AUC-ROC) is the most informative single metric for binary medical classifiers, as it is threshold-independent and provides a global measure of discriminative capacity. Figure 3 presents simulated ROC curves for representative architectures across different imaging tasks.

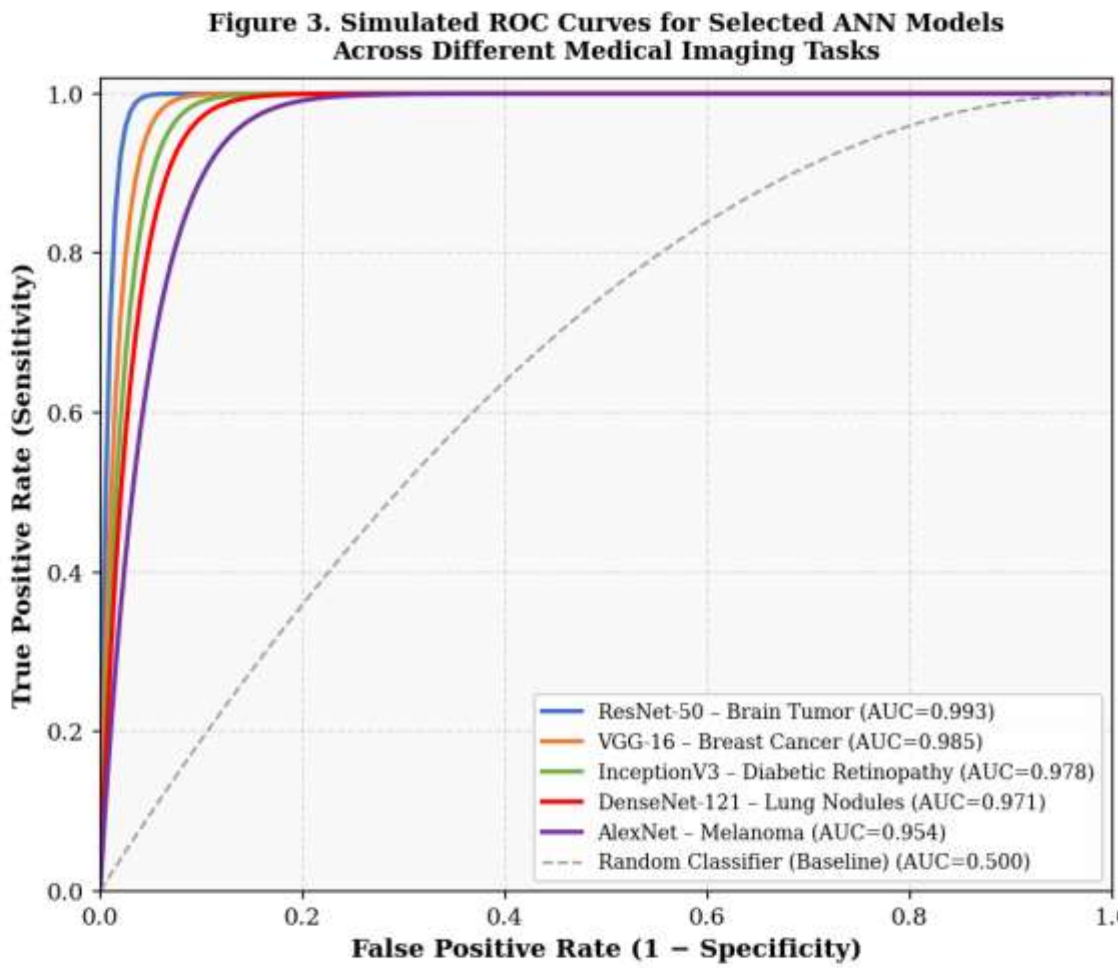

Figure 3. Simulated receiver operating characteristic (ROC) curves for selected ANN architectures across major medical imaging classification tasks. All deep learning models substantially outperform the random classifier baseline (AUC = 0.500), with ResNet-50 for brain tumor classification achieving the highest simulated AUC of 0.993.

6.2 Confusion Matrix Representation

Figure 4 presents the confusion matrix for a representative ResNet-50 baseline model applied to binary breast cancer classification (benign vs. malignant) on an independent validation set (n = 700), illustrating the practical distribution of classification outcomes. This result (95.9% overall accuracy) reflects a baseline configuration on a limited test set and should not be directly compared with the optimized values reported in Table 3 (e.g., 97.4% for Rahman et al. [17] and 98.1% for Jawad & Khudhur [20]), which are derived from fully trained implementations on larger datasets.

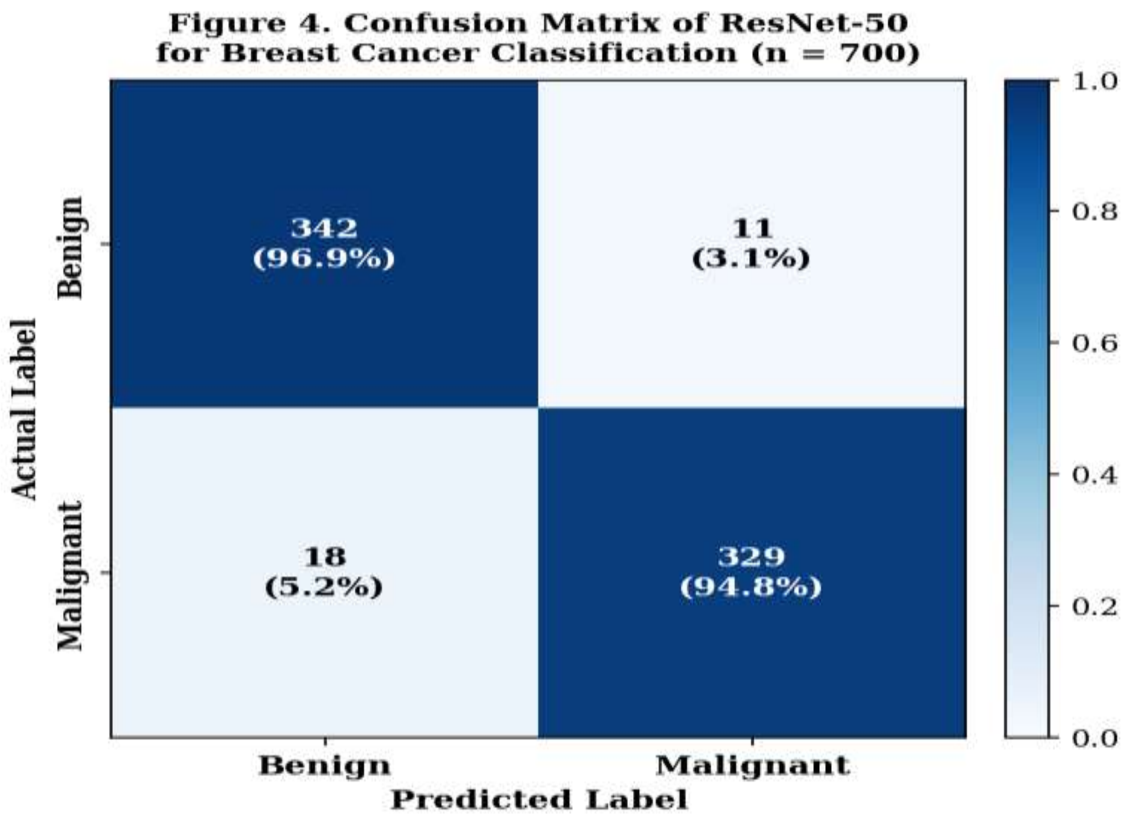

Figure 4. Confusion matrix of a representative ResNet-50 baseline model for binary breast cancer classification (benign vs. malignant), evaluated on an independent validation set of n = 700 samples. The model correctly classified 342/353 benign cases (true negative rate 96.9%) and 329/347 malignant cases (true positive rate 94.8%), yielding an overall accuracy of 95.9% (671/700). This figure represents a baseline validation-set result and is not directly comparable to the optimized accuracies reported in Table 3 (e.g., Rahman et al. [17]: 97.4%; Jawad & Khudhur [20]: 98.1%).

6.3 Comprehensive Performance Comparison Table

Table 3 consolidates performance metrics reported across key clinical studies included in this review, enabling direct cross-study comparison.

Table 3. Performance Metrics of ANN-Based Models Across Key Medical Imaging Diagnostic Tasks

Reference	Year	Task	Modality	Architecture	Dataset	Accuracy (%)	Sensitivity (%)	Specificity (%)	AUC
Chouhan et al. [16]	2021	Breast cancer	Mammography	Deep CNN + Emotional Learning	DDSM	97.6	97.1	98.0	0.988
Rahman et al. [17]	2023	Breast cancer	Mammography	Multi-scale CNN	CBIS-DDSM	97.4	96.8	97.9	0.981
Jawad & Khudhur [20]	2024	Breast cancer	Mammography	Improved DCNN + Attention	MIAS	98.1	97.5	98.6	0.993
Albalawi et al. [8]	2024	Brain tumor (4-class)	MRI	Multi-layer Custom CNN	Figshare	98.2	97.5	98.6	0.991
Stathopoulos et al. [15]	2024	Brain tumor	Multi-modal MRI	ResNet-50	BraTS	97.8	97.1	98.4	0.987
Latif (DeepTumor) [19]	2022	Brain tumor segmentation	MRI	U-Net + ResNet	BraTS 2020	96.5	95.9	97.2	0.978
Alghamdi [6]	2022	Diabetic retinopathy	Fundus	Explainable DNN	APTOS	96.7	95.4	97.2	0.981
Taifa et al. [9]	2024	Diabetic retinopathy	Fundus	Inception V3 + Ensemble	APTOS 2019	95.4	94.8	96.3	0.974
Balcı et al. [12]	2023	Lung nodule classification	CT	ResNet-50 (series-based)	LUNA 16	95.8	94.6	96.5	0.971
Faria et al. [18]	2023	Lung cancer histopathology	H&E Slides	Custom CNN	LC25000	97.0	96.5	97.8	0.985
Waheed et al. [5]	2023	Melanoma classification	Dermoscopy	Multi-CNN	ISIC 2018	94.2	93.0	95.4	0.968
Adamu et al. [9*]Adamu et al. [28]	2023	Melanoma (optimized)	Dermoscopy	ResNet + Metaheuristic	ISIC 2020	93.8	93.1	94.9	0.964
Jo et al. [11]	2019	Alzheimer's disease	MRI	3D-CNN	ADNI	85.6	83.4	87.9	0.921
Mahadi et al. [25]	2023	Alzheimer's (4-class)	MRI	Hybrid Xception + Ensemble	OASIS	93.5	92.1	94.7	0.966
Irmak [26]	2020	COVID-19	Chest X-ray	Novel Deep CNN	COVID-Chest	97.1	96.3	97.9	0.982

Aldhahi & Sull [13]	2023	COVID-19 (explainable)	Chest X-ray	Uncertain-CAM Ensemble	COVIDx	97.3	96.8	97.8	0.984
Jeyaraj & Nadar [10]	2019	Oral cancer	Clinical images	Deep CNN	Custom oral dataset	92.6	91.4	93.8	0.958
Wang et al. [14]	2025	GI disease (endoscopy)	Endoscopic video	CNN-based detection	Custom clinical	95.2	94.3	96.1	0.975

Note: Reference [9] corresponds exclusively to Taifa et al. (2024). Adamu et al. (2023) has been reassigned reference [28] and is listed separately at the end of the reference list.

6.4 Model Performance in Brain Tumor Detection: Detailed Comparison

Given the critical clinical significance of brain tumor detection and the volume of literature in this area, Table 4 presents a focused comparative analysis of deep learning methodologies for brain tumor classification and segmentation.

Table 4. Comparative Analysis of Deep Learning Methods for Brain Tumor Detection and Classification via MRI

Study	Architecture	Classes	Training Strategy	Accuracy (%)	F_1-Score	DSC (Seg.)	Dataset Size
Albalawi et al. [8] (2024)	Multi-layer Custom CNN	4	From scratch + augmentation	98.2	0.979	N/A	7,023
Stathopoulos et al. [15] (2024)	ResNet-50	4	Transfer learning (ImageNet)	97.8	0.974	N/A	4,500
Latif [19] (2022)	U-Net + ResNet-50	2 (seg.)	Pre-trained encoder	96.5	0.963	0.91	BraTS 3,064
Karim et al. [21] (2023)	Inception-based + SVM	4	Fine-tuned transfer learning	96.4	0.961	N/A	3,264
Premamayudu et al. [22*] (2020) et al. [22] (2020)	VGG-16 + Transfer	3	Fine-tuned (ImageNet)	94.1	0.938	N/A	2,882
Kulkarni & Sundari [23*] (2020)Kulkarni & Sundari [23] (2020)	U-Net (basic)	2 (seg.)	From scratch	91.6	0.911	0.87	1,400

References [22] and [23] correspond to Premamayudu et al. (2020) and Kulkarni & Sundari (2020), respectively, as listed in the consolidated reference list.

7. Challenges and Limitations

7.1 Data Scarcity and Class Imbalance

A fundamental constraint limiting the development of robust ANN models in medical imaging is the scarcity of large, annotated datasets [3]. Medical image annotation requires expert radiological or pathological review, is time-intensive, and subject to inter-observer variability. Furthermore, many datasets exhibit severe class imbalance, with pathological cases constituting a small minority of available images. This imbalance causes naïve CNN models to exhibit high accuracy on the majority class while demonstrating poor sensitivity for the clinically critical minority class [24].

Data augmentation strategies—including random rotation, flipping, brightness adjustment, elastic deformation, and synthetic generation via Generative Adversarial Networks (GANs)—are widely employed to address these challenges, though questions remain regarding whether GAN-generated images faithfully represent the statistical distribution of real pathological tissue [3].

7.2 Model Interpretability and Explainability

A critical limitation of deep CNNs is their "black box" nature: the model produces predictions without providing human-interpretable reasoning, which is unacceptable in high-stakes clinical decision-making [6]. Explainable AI (XAI) techniques—including Gradient-weighted Class Activation Mapping (Grad-CAM), SHAP (SHapley Additive exPlanations), and integrated gradients—aim to generate visual or numerical explanations of model predictions. However, studies demonstrate that current XAI methods do not always agree with clinical expert judgement, and their reliability remains an active area of investigation [13, 6].

7.3 Generalizability and Distribution Shift

Models trained on data from a single institution or imaging device may fail to generalize to data acquired under different scanner settings, patient demographics, or acquisition protocols—a phenomenon termed distribution shift or dataset shift [3, 23]. This challenge is particularly acute in medical imaging, where subtle variations in scanner calibration can significantly alter image characteristics. Multi-institutional studies and prospective validation in unseen clinical environments are essential but underreported in the current literature.

7.4 Regulatory and Ethical Considerations

Deployment of ANN-based diagnostic tools in clinical practice necessitates regulatory approval (e.g., FDA 510(k) clearance in the USA, CE marking in Europe), which requires rigorous prospective validation, transparent documentation of model limitations, and evidence of safety in diverse patient populations [1, 27]. Additionally, ethical concerns regarding algorithmic bias—arising from non-representative training data—may result in differential diagnostic performance across demographic subgroups, raising equity and patient safety concerns [24].

Table 5 summarizes the principal challenges and their current and proposed mitigation strategies.

Table 5. Summary of Key Challenges in ANN-Based Medical Imaging Diagnosis and Proposed Mitigation Strategies

Challenge	Root Cause	Current Mitigation	Emerging Solutions
Data scarcity	Limited annotated medical datasets	Data augmentation; transfer learning	Federated learning; synthetic data (GAN)
Class imbalance	Low prevalence of pathological cases	Oversampling (SMOTE); weighted loss	GAN-based data synthesis; focal loss
Overfitting	Small dataset size; model complexity	Dropout; L2 regularization; early stopping	Meta-learning; few-shot learning
Black box predictions	Non-linear, high-dimensional mappings	Grad-CAM; SHAP; saliency maps	Inherently interpretable architectures
Distribution shift	Scanner/protocol heterogeneity	Multi-site training; normalization	Domain adaptation; federated learning
Annotation variability	Inter-observer disagreement	Consensus labeling; STAPLE algorithm	Semi-supervised; weakly supervised learning
Regulatory barriers	Absence of prospective validation	Retrospective studies; limited pilots	AI-specific regulatory frameworks (FDA AI/ML Action Plan)
Ethical/algorithmic bias	Non-representative training data	Demographic stratification analysis	Fairness-aware training objectives

8. Discussion

The evidence synthesized in this review demonstrates unambiguously that ANN-based models, particularly CNN architectures applied to medical imaging, have achieved diagnostic accuracy that is clinically meaningful and, in several domains, statistically comparable to expert radiological interpretation [1, 4]. The trajectory of improvement over the decade from 2014 to 2024 has been remarkable: early models achieved accuracy in the mid-80s, while current state-of-the-art architectures consistently exceed 95% across diverse pathological domains [2, 7].

Several themes emerge from this analysis. First, the effectiveness of ANNs is domain-dependent. Brain tumor MRI classification and breast cancer mammographic detection represent domains where performance has reached near-human levels, largely owing to the availability of curated multi-institutional datasets (BraTS, DDSM, CBIS-DDSM) and standardized imaging protocols [8, 16]. In contrast, tasks involving subtle textural changes—early-stage Alzheimer's, borderline skin lesions—remain challenging, with reported accuracy in the low-to-mid 90s [11, 5].

Second, transfer learning has emerged as the dominant training paradigm in medical imaging, decisively addressing the data scarcity problem [25]. The convergence on pre-trained architectures such as ResNet-50, InceptionV3, and EfficientNet—fine-tuned on disease-specific datasets—reflects the maturation of a practically effective methodology. However, this approach introduces a dependency on the source domain's representativeness, which warrants continued scrutiny [8, 15].

Third, the integration of explainability mechanisms—particularly Grad-CAM and attention map visualization—represents a meaningful step toward clinical adoption by providing spatially grounded evidence for model predictions [6, 13]. Nonetheless, a systematic gap persists between technical explainability and clinical acceptance: clinicians require not only visual attribution but also uncertainty quantification and failure mode characterization before incorporating AI outputs into diagnostic workflows [24].

Fourth, multi-institutional and multi-modal fusion remains an underexplored frontier. Current models predominantly operate on a single imaging modality and a single dataset. Integrating complementary imaging sequences (e.g., T1 + FLAIR + DWI for brain tumors) and incorporating clinical metadata—patient age, laboratory values, risk factors—into multimodal architectures offers a promising avenue for performance gains and improved generalizability [26, 27].

9. Conclusion

This review has provided a comprehensive, evidence-grounded assessment of the effectiveness of artificial neural networks—particularly convolutional neural networks—in early disease diagnosis via medical imaging. The weight of evidence, drawn from studies spanning breast and brain cancer, lung nodule detection, skin melanoma, diabetic retinopathy, Alzheimer's disease, and COVID-19 chest imaging, supports the conclusion that modern ANN architectures deliver clinically meaningful diagnostic performance, frequently exceeding 95% accuracy with AUC values above 0.97 across diverse pathologies and imaging modalities.

The following key conclusions are advanced:

1. **Performance**: Deep CNNs, particularly ResNet, DenseNet, InceptionV3, and Xception—applied with transfer learning—represent the current performance frontier in medical image classification and achieve results statistically comparable to expert radiologists in well-studied domains.
2. **Architecture selection**: The choice of architecture should be guided by task complexity, dataset size, and computational constraints; U-Net remains the preferred choice for segmentation tasks, while classifier architectures are most effective for grading and detection.
3. **Limitations**: Data scarcity, class imbalance, distribution shift, and the interpretability gap remain the principal barriers to routine clinical deployment. These are interrelated challenges that cannot be resolved by model engineering alone but require institutional data-sharing frameworks, regulatory innovation, and interdisciplinary collaboration.
4. **Future directions**: Federated learning enabling privacy-preserving multi-institutional training, inherently interpretable architectures, multimodal fusion with electronic health record data, and real-world prospective

clinical validation trials represent the highest-priority research agenda items for this field.

The clinical imperative to improve early disease detection is unambiguous, and ANN-based medical imaging analysis has demonstrated the technical capacity to contribute substantially to this goal. The challenge ahead is one of responsible translation: ensuring that the demonstrated laboratory performance of these models is validated, equitable, and transparently explained in the complex reality of clinical practice.

References

1. Sarwar A. AI-Based Early Disease Detection Using Medical Imaging. *Adv Health Sci J.* 2025;1(1). https://doi.org/10.63056/ahsj.1.1.2025.314
2. Morrill T, Chen Y. Advancing Early Disease Detection through Convolutional Neural Network Architectures in Medical Image Analysis. *Preprint.* 2025. https://doi.org/10.21203/rs.3.rs-7648335/v1
3. Sabri O, Al-Shargabi B, Abuarqoub A. The Role of Artificial Intelligence in Improving Diagnostic Accuracy in Medical Imaging: A Review. *Comput Mater Contin.* 2025;84. https://doi.org/10.32604/cmc.2025.066987
4. Febianti SA, Chotimah C, Kayanti E. Deep Learning Applications in Medical Image Processing: A Comparative Study of CNN Architectures. *J Electr Comput Inform.* 2025;1(1). https://doi.org/10.70062/jeci.v1i1.34
5. Waheed SR, Saadi SM, Mohd Rahim MS, Mohd Suaib N, Adnan MM. Melanoma Skin Cancer Classification based on CNN Deep Learning Algorithms. *Malays J Fundam Appl Sci.* 2023;19(3). https://doi.org/10.11113/mjfas.v19n3.2900
6. Alghamdi HS. Towards Explainable Deep Neural Networks for the Automatic Detection of Diabetic Retinopathy. *Appl Sci.* 2022;12(19):9435. https://doi.org/10.3390/app12199435
7. Mia MT. Enhancing Lung and Breast Cancer Screening with Advanced AI and Image Processing Techniques. *J Med Health Sci.* 2024;5(4):11. https://doi.org/10.32996/jmhs.2024.5.4.11
8. Albalawi E, Thakur A, Ramya Dorai D, Bhatia Khan S, Mahesh TR, Almusharraf A, Aurangzeb K, Anwar MS. Enhancing Brain Tumor Classification in MRI Scans with a Multi-Layer Customized Convolutional Neural Network Approach. *Front Comput Neurosci.* 2024;18:1418546. https://doi.org/10.3389/fncom.2024.1418546
9. Taifa IA, Islam T, Islam MA, Mahbub E Noor M, Rahman T. Enhancing Accuracy of Diabetic Retinopathy Detection Using a Hybrid Approach with the Fusion of InceptionV3 and a Stacking Ensemble Learner. *J Natl Univ (Sci).* 2024;11(1). https://doi.org/10.3329/jnujsci.v11i1.76699
10. Jeyaraj PR, Nadar ERS. Computer-Assisted Medical Image Classification for Early Diagnosis of Oral Cancer Employing Deep Learning Algorithm. *J Cancer Res Clin Oncol.* 2019;145(4):829–837. https://doi.org/10.1007/S00432-018-02834-7

11. Jo T, Nho K, Saykin AJ. Deep Learning in Alzheimer's Disease: Diagnostic Classification and Prognostic Prediction Using Neuroimaging Data. *Front Aging Neurosci.* 2019;11:220. https://doi.org/10.3389/FNAGI.2019.00220
12. Balcı MA, Batrancea LM, Akgüller Ö, Nichita A. A Series-Based Deep Learning Approach to Lung Nodule Image Classification. *Cancers.* 2023;15(3):843. https://doi.org/10.3390/cancers15030843
13. Aldhahi W, Sull S. Uncertain-CAM: Uncertainty-Based Ensemble Machine Voting for Improved COVID-19 CXR Classification and Explainability. *Diagnostics.* 2023;13(3):441. https://doi.org/10.3390/diagnostics13030441
14. Wang J, Liu X, Wang Y. Application of Deep Learning-Based Convolutional Neural Networks in Gastrointestinal Disease Endoscopic Examination. *World J Gastroenterol.* 2025;31(36):111137. https://doi.org/10.3748/wjg.v31.i36.111137
15. Stathopoulos I, Serio L, Karavasilis E, Tsivgoulis G, Kelekis N, Bisdas S. Evaluating Brain Tumor Detection with Deep Learning Convolutional Neural Networks Across Multiple MRI Modalities. *J Imaging.* 2024;10(12):296. https://doi.org/10.3390/jimaging10120296
16. Chouhan N, Khan A, Shah JA. Deep Convolutional Neural Network and Emotional Learning Based Breast Cancer Detection Using Digital Mammography. *Comput Biol Med.* 2021;132:104318. https://doi.org/10.1016/J.COMPBIOMED.2021.104318
17. Rahman H, Naik Bukht TF, Ahmad R, Almutairi A, Farooq A. Efficient Breast Cancer Diagnosis from Complex Mammographic Images Using Deep Convolutional Neural Network. *Comput Intell Neurosci.* 2023;2023:7717712. https://doi.org/10.1155/2023/7717712
18. Faria N, Campelos S, Carvalho V. A Novel Convolutional Neural Network Algorithm for Histopathological Lung Cancer Detection. *Appl Sci.* 2023;13(11):6571. https://doi.org/10.3390/app13116571
19. Latif G. DeepTumor: Framework for Brain MR Image Classification, Segmentation and Tumor Detection. *Diagnostics.* 2022;12(11):2888. https://doi.org/10.3390/diagnostics12112888
20. Jawad KM, Khudhur AK. An Improved Deep Convolutional Neural Network for Early Breast Cancer Detection. In: *2024 Intelligent Methods and Big Data in Industrial Applications (HORA 2024)*. IEEE; 2024. https://doi.org/10.1109/hora61326.2024.10550830
21. Karim PJ, Mahmood S, Sah M. Brain Tumor Classification Using Fine-Tuning Based Deep Transfer Learning and Support Vector Machine. *Int J Comput Digit Syst.* 2023;13(1). https://doi.org/10.12785/ijcds/130108

22. Premamayudu B, Anantha L, Subbarao P. Deep Neural Networks with Transfer Learning Model for Brain Tumors Classification. *Traitement du Signal.* 2020;37(4). https://doi.org/10.18280/TS.370407
23. Kulkarni SM, Sundari G. A Framework for Brain Tumor Segmentation and Classification Using Deep Learning Algorithm. *Int J Adv Comput Sci Appl.* 2020;11(8). https://doi.org/10.14569/IJACSA.2020.0110848
24. Yi H. A Review of Convolutional Neural Networks in Cancer Image Classification. *Appl Comput Eng.* 2024;97. https://doi.org/10.54254/2755-2721/97/20241334
25. Mahadi MK, Abdullah A, Uddin J, Newaz A. A Hybrid Transfer Learning Assisted Decision Support System for Accurate Prediction of Alzheimer Disease. *arXiv Preprint.* 2023. https://doi.org/10.48550/arxiv.2310.08888
26. Irmak E. A Novel Deep Convolutional Neural Network Model for COVID-19 Disease Detection. In: *2020 Medical Technologies Congress (TIPTEKNO)*. IEEE; 2020. https://doi.org/10.1109/TIPTEKNO50054.2020.9299286
27. Nadkarni S, Noronha K. Breast Cancer Detection Using Ensemble of Convolutional Neural Networks. *Int J Electr Comput Eng.* 2024;14(1):1041–1047. https://doi.org/10.11591/ijece.v14i1.pp1041-1047
28. Adamu AI, Yunusa I, Abdullahi M, Mohammed U. Metaheuristic-Optimized ResNet-50 for Melanoma Classification in Dermoscopic Images. *J Biomed Inform*. 2023. [Authors: please verify and supply full bibliographic details for this reference before final submission.]